Energy and Environmental Systems Group
Institute for Sustainable Energy, Environment and Economy (ISEEE)

Geomechanical Analysis

Wabamun Area CO_2 Sequestration Project (WASP)

Author

Runar Nygaard

Rev.	Date	Description	Prepared by
1	January 8, 2010	Geomechanical Analysis	Runar Nygaard

Table of Contents

List of Tables

List of Figures

INTRODUCTION

To minimize the potential for CO_2 leakage during and after injection, a geomechanical assessment must be performed to determine the potential for fracturing and faulting caused by the injection process. Potential CO_2 leakage paths can be controlled using geomechanical parameters, such as in-situ stress, rock stiffness and rock strength. It can also be controlled by sealing the top of the formation. When selecting a storage site, major existing faults and fractures should be avoided and proper injection procedures should be followed to reduce the likelihood of CO_2 leakage.

The first phase of the geomechanical assessment was to establish the properties of the formation, including rock stiffness and rock strength, as well as determining the in-situ conditions. The second phase of the assessment was to perform numerical analyses using the findings from the first phase. Those findings have been provided in the Geomechanical Modelling section of this report.

The purpose for studying the geomechanical properties of the injection site is to ensure seal integrity during and after CO_2 injection. To conduct a geomechanical characterization, we need to obtain stress and pressure information and geomechanical information, such as strength and deformation properties of the injection horizon and caprock.

In this project, no new wells were drilled and therefore no recently captured and undisturbed cores were available for geomechanical testing. It was therefore decided to base the geomechanical characterization on data obtained from downhole logging tools. This approach is a well established method used in the oil and gas industry. The characterization of rock properties for this area was recently studied by Haug et al (2008), and this report is an expansion of that work. In-situ stress has also been extensively studied for the area, so no new significant data was available for the project. Therefore, the in-situ stress analysis is based on previously published material for the area.

1. DOWN HOLE GEOLOGICAL MODEL

The geological study of the Nisku formation defined the site as a likely injection horizon for CO_2 and as a result, the geomechanical work concentrated on establishing the properties of the Nisku aquifer formation and identified aquitards (non-flowing) formations higher in the subsurface. Figure 1 shows the stratigraphy in the Wabamun Lake area above the Nisku formation. The sedimentary succession is divided by the thick Colorado Group shale aquitard and two main hydrostratigraphic groups—the Upper Devonian-Lower Cretaceous and the post-Colorado. Each major group contains several aquifers and intervening aquitards. The Nisku Formation is part of the Upper Devonian-Lower Cretaceous hydrostratigraphic group and is capped by the overlying Calmar formation aquitard.

The Nisku formation is on average 72 metres thick and typically ranges from approximately 60 to 98 metres, but thins to less than 40 metres in the northwest. It is capped by the Calmar Formation shale ranging in thickness from 5 to 15 metres. The caprock is overlain by the upper Devonian-Lower Cretaceous aquifers (> 500 metres). Ultimately, the thickness of the Colorado and Lea Park aquitards (> 500 metres) above them would act as a final barrier to any vertically migrating CO_2. The Devonian-Lower Cretaceous aquifer system, however, contains several oil and gas field in the area. To prevent CO_2 from migrating towards existing petroleum production, it is important to determine if the Calmar may be breached during or after injection.

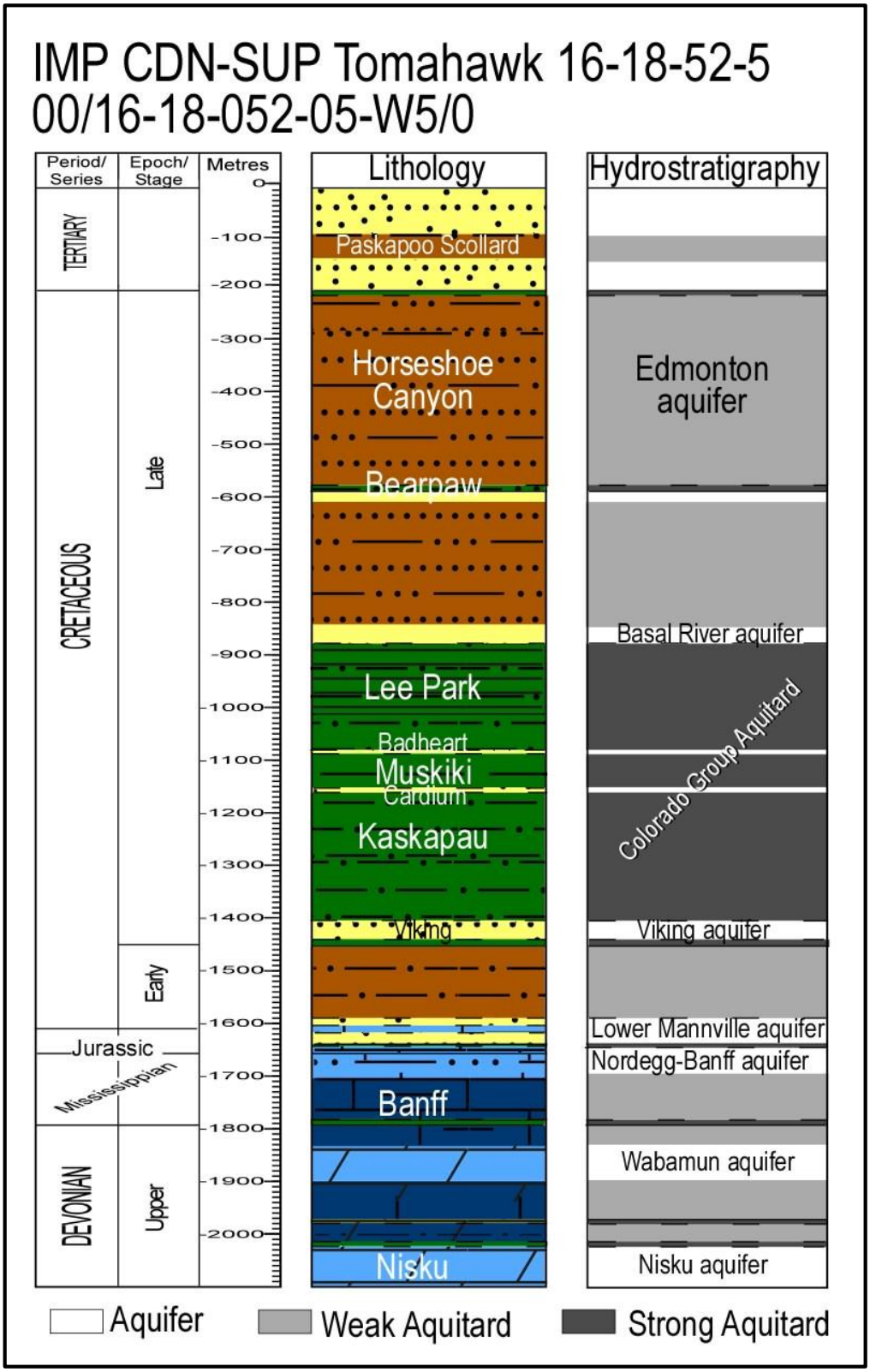

Figure 1: Downhole model shows the stratigraphic succession for the Wabamun Lake study area, from the Upper Devonian to the surface (from Haug et al, 2008).

2. IN-SITU STRESS

2.1 In-situ Stress Methodology

In the subsurface, the underground formation has to carry the weight of the overlying rock. The vertical stress (S_v) at any point in the underground is equivalent to the weight of the overburden. Integration of a bulk density log conducted while the well was logged after it was drilled provides the vertical stress at depth (D), with the stress derived from the formula:

$$Sv = \int \rho \mathbf{b}(\mathbf{z}) \mathbf{g} \mathbf{d} \mathbf{z} \qquad [1]$$

where $\rho_b(z)$ is the bulk density of the fluid-saturated rock, which changes with the depth according to the density logs. The gravity constant is g. In most wells there is an upper interval that is unlogged, and an average density for the rock in this unlogged interval has been assumed. Since the rock is porous, it will be filled with fluids. The fluid pressure can be calculated similar to the equation for vertical stress, but instead integrating fluid density.

The z-axis in the equation above is vertical with z = 0, which corresponds to the earth's surface. Since there is no shear stress acting at the surface, the vertical stress is one of the principal stresses (when the earth surface is completely flat). The stress in the underground consists of three mutually orthogonal principal stresses with two horizontal and oriented 90° apart. The two horizontal stresses often deviate in magnitude from each other with the largest horizontal stress denoted as SH_{max} and the least horizontal stress SH_{min}. Due to geological events, such as tectonic activity and push from mountains, the SH_{max} (as well as SH_{min}) can be larger than the vertical stress.

The minimum horizontal stress magnitude can be evaluated using a variety of tests. The most accurate method for determining SH_{min} is through micro-fracture testing, where a wellbore is carefully fractured by injecting fluids into a small portion of the open hole. Mini-fracturing, leak-off tests and fracture breakdown pressures can also be used to estimate the horizontal stress (Bell, 2003; Bell and Bachu, 2003). Estimating the minimum horizontal stress (SH_{min}) in a well provides the lower limit of the fracturing pressure and puts a limit on the allowable injection pressure in a well.

The SH_{min} orientation can be determined from borehole breakouts, which are spalled cavities that occur on opposite walls of a borehole in the SH_{min} orientation, or from tensile fractures with orientation parallel to the SH_{max} (Bell, 2003).

2.2 WASP In-Situ Stress Field

The reported S_v gradient in the area is 23 kPa/m (see Figure 2). The average gradient SH_{min} in the Wabamun Lake study area is 20 kPa/m (Michael et al, 2008). These two stress gradients (S_v and SH_{min}) provide loose lower and upper bounds for the fracturing pressure gradient, which was generally found to be ~ 19 kPa/m for the entire Alberta basin (Bachu et al, 2005).

The direction of SH_{min} was approximately 145° in a general southeast-northwest direction. This means that fractures will form and propagate in a vertical plane in a southwest-northeast direction (~ 55°), essentially perpendicular to the Rocky Mountain deformation front. Regional scale studies of the stress regime indicate that in south and central Alberta, vertical stress (S_v) is the largest principal stress and is greater than the maximum horizontal stress (SH_{max}) (Bell and Bachu, 2003).

Since the reported breakouts have a distinct orientation, SH_{max} will be higher than the horizontal stress. These two data points constrain SH_{max} at a value higher than 20, but lower than 23 kPa/m, which roughly corresponds to a value of around 21 to 22 kPa/m.

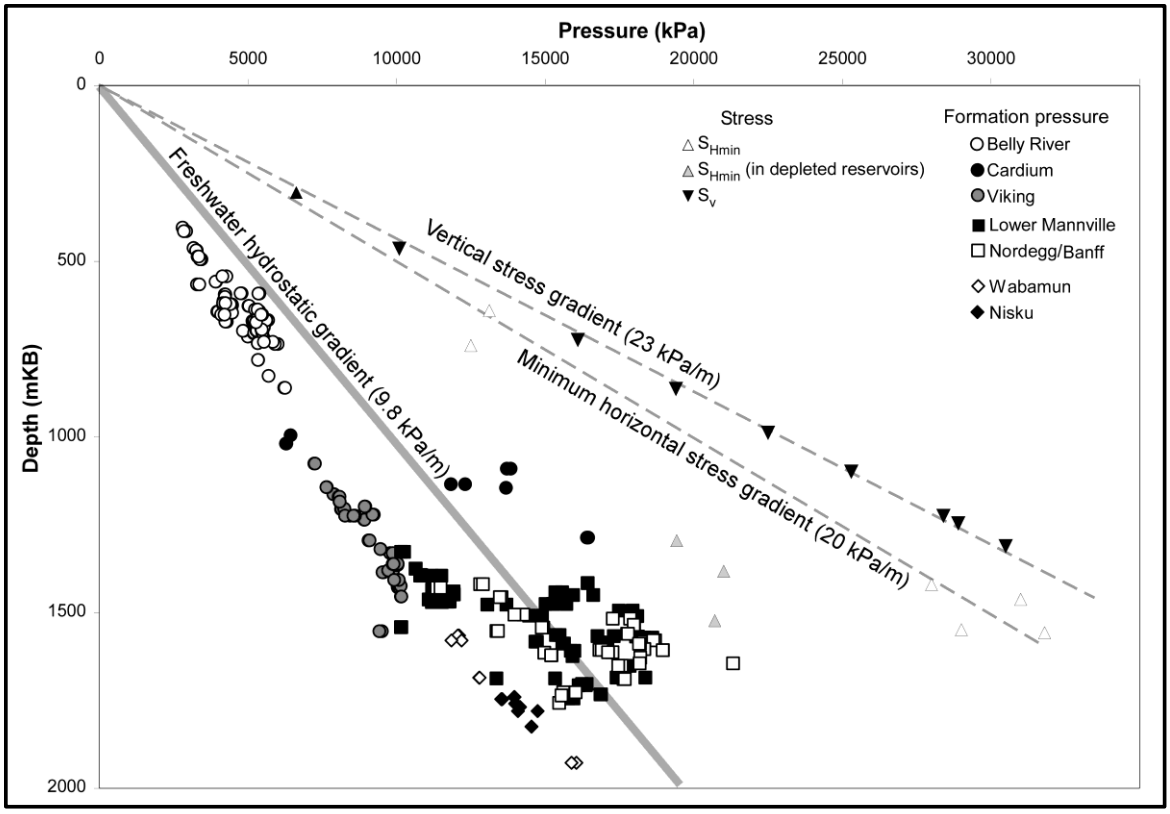

Figure 2: Vertical and least horizontal stress and pore pressure gradients (Michael et al, 2008).

Table 1: WASP area stress gradients and stress orientations.

	Vertical Stress (MPa/km)	Largest Horizontal Stress (MPa/km)	Least Horizontal Stress
Magnitude	23	~ 22 (20–23)	20
Orientation	Vertical	55° (NE)	145° (SE)

3. GEOMECHANICAL ROCK PROPERTIES

3.1 Methodology for Establishing Geomechanical Rock Properties

In this project there were no new wells drilled, and therefore no recently captured and preserved core samples to evaluate. As a result, the geomechanical characterization study was based on data obtained from downhole logging tools. The geomechanical characterization of rock properties in this area was recently studied by Haug et al (2008). This report expands on this previous work.

The most comprehensive and accurate method for establishing geomechanical information on the strength and deformation of a material is by conducting rock mechanical laboratory tests of the preserved core material. Core material is hard to find for most overburden formations and water-

filled reservoirs. This is especially true in the early phases of a storage project, where localization has not been finalized and detailed engineering work not yet started. However if laboratory tests are performed, they only represent a single point in a formation without taking into account spatial variations in geomechanical parameters. This means that indirect measurements of these properties will have to be used to obtain rock strength and deformation properties. This approach is a well-established method used in the oil and gas industry for similar types of analyses, such as caprock integrity, wellbore stability and sand production.

With a lack of laboratory measurements for deformation properties, the properties will have to be obtained from well logs. Dynamic elastic properties, such as Poisson's ratio and Young's modulus, can be calculated using wireline logs. The Poisson's ratio and Young's modulus are determined from P- and S-wave velocity (sonic) and density logs. The dynamic Poisson's ratio (v_d) is calculated from the relationship between the P-wave velocity (V_p) and S-wave velocity (V_s) as:

$$v_d = \frac{V_P^2 - 2V_S^2}{2(V_P^2 - V_S^2)} \quad [2]$$

The Elastic Young's modulus can be calculated from velocity and rock density logs based on:

$$E_d = 2\rho * V_S^2 (1 - \upsilon_d) \quad [3]$$

where E_d is dynamic Young's modulus (GPa), ρ is rock density (g/cm^3), V_s is shear velocity and v_d is dynamic Poisson's ratio calculated based on Equation 2. Dynamic Poisson's ratio is a good approximation to the static dynamic modulus. However in a velocity measurement, the strain rate varies from about 10^{-2} to 10^{-4} s^{-1} and has a maximum strain of 10^{-6} while rock mechanical tests, which measure static deformation properties, are conducted at a strain rate of 10^{-2} s^{-1} and a maximum strain of 10^{-2}. The variation in strain and strain rate causes the moduli calculated using dynamic measurements to be higher than moduli calculated based on static measurements conducted in a laboratory. Based on the following correlation from Haug et al (2008) between unconfined compressive strength (UCS) and static Young's module:

$$E_s = 111 * UCS^{1.2} \quad [4]$$

where E_s is static Young's module (in GPa) and UCS (in MPa) is the ratio between dynamic and static Young's module. The ratio was determined to be 2.7:1, and the conversion factor was used for all formations to convert dynamic to static Young's module values. The bulk modulus, which is a function of Poisson's ratio and Young's module, is reported as well.

Two distinctly different modes can cause rock to fail. One is when the stress on the rock reaches the critical limit in tension and the rock is pulled apart (e.g., during hydraulic fracturing of a wellbore), and the second is when shear stress is above a critical level and a shear plane is created. The critical limit for tensile failure is tensile strength, and the critical limit for shear strength is the cohesive strength or unconfined compressive strength. The unconfined compressive strength is the force required to break the rock when compressed without any side support.

The use of sonic velocity logs to determine unconfined compressive rock strength is well established. There exists several correlations between rock strength and sonic travel time or a combination of different logs (e.g., Kasi et al, 1983; Onyia, 1988; Hareland and Nygaard 2007; Andrews et al, 2007). Onyia (1988) conducted laboratory tri-axial compressive tests from different

lithologies to develop a continuous log-based rock strength based on wireline compressional sonic travel. The experimental relationship for calculating unconfined compressive strength that Onyia established is given in Equation 5:

$$UCS = \left(\frac{1.00}{k_1 (\Delta t_c - k_2)^{k_3}} \right) + k_4 \qquad [5]$$

where Δt_c is travel time in μs/ft, UCS is sonic-based unconfined compressive, and k_1, k_2, k_3 and k_4 are lithology dependant constants (see Table 2). In this study we used correlations on limestone and dolomites from Onyia's work. For shales and sandstones, the unconfined compressive strength laboratory results and sonic log data from Hareland and Nygaard (2007) were used to derive the lithology dependant constants used in Equation 5. In addition to the shale and sandstone correlations, a combined (combo) shale and sandstone correlation was derived from the same dataset to be used for shaly sandstones and sand-rich shales. Gamma ray log readings were used to distinguish between the clastic lithologies, and the sandstone correlation was used for all gamma ray readings below 40 API units, shale correlation were used for all gamma ray readings above 110 API units, and the combined correlation was used for all readings in between.

Figure 3 shows the correlations between UCS and sonic travel time from wireline log data for the different lithologies. The correlations are derived based on rock mechanical tests with reported UCS values in the range of 8 to 120 MPa.

Table 2: Lithological dependant regression constants for UCS determination based on the sonic log correlation in Equation 5.

Lithology	Limestone	Dolomite	Sandstone	Shale	Combo
k1	8.07E-06	1.65E-04	2.48E-06	1.83E-05	1.34E-05
k2	23.87	0	23.87	23.87	23.87
k3	2	1	2.35	1.80	1.92
k4	0.014	20.99	0	0	0

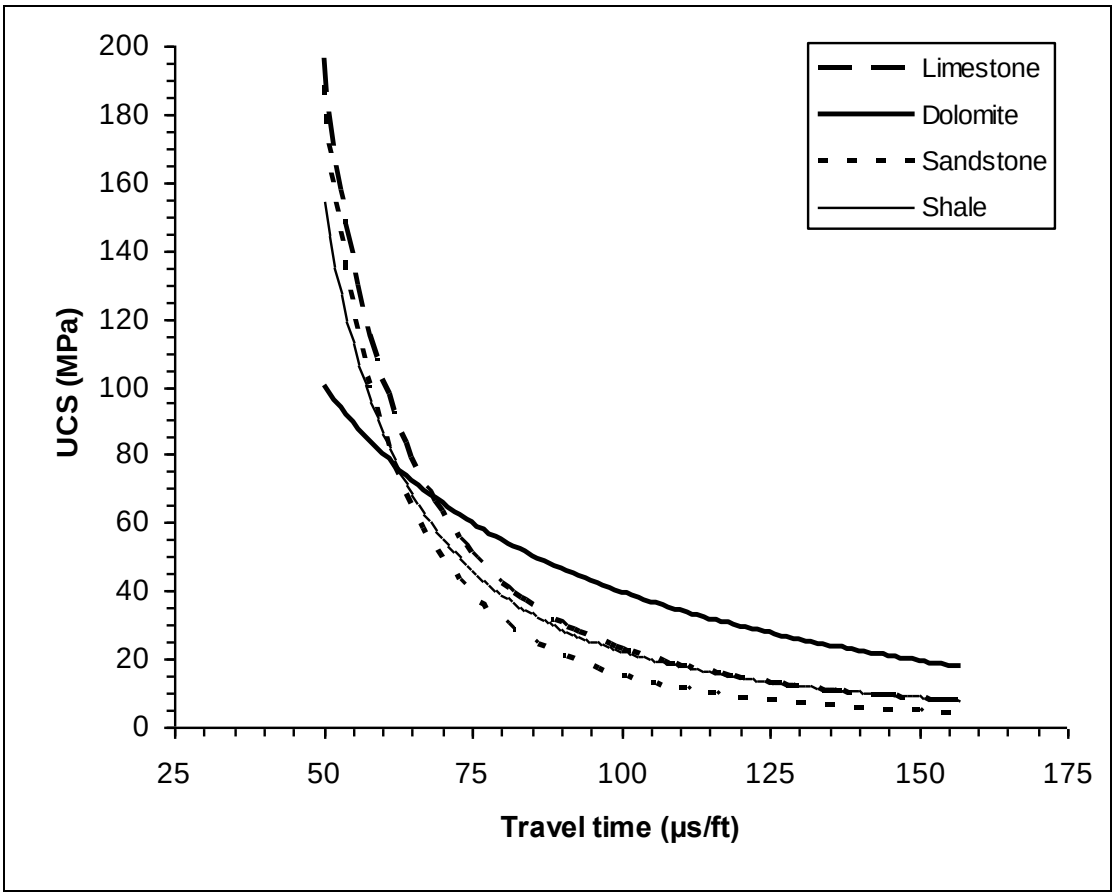

Figure 3: Correlations between unconfined compressive rock strength (UCS) and p-wave sonic travel time from wireline logs (Hareland and Hareland, 2007).

In the subsurface the rock has side support from horizontal stress, which makes the rock appear stronger in the subsurface due to the horizontal stress support. To determine the confined strength, tests can be conducted at different confining stress points with the test results plotted as a function of confining stress. From this a failure line can be drawn. The angle of this line is the failure angle. Another method is to report the failure data in Mohr-Coulomb failure criteria in shear stress and mean stress space where the failure line is determined by cohesion and friction angle. Both sets of values are reported.

3.2 Table of Geomechanical Properties

When characterizing the geomechanical properties of geological formations, the formations are combined into similar geomechanical units (GMU). This is done to reduce the amount of data that needs to be distributed into a geomechanical simulation at a later stage. It also helps reduce the complexity of the geomechanical model and computational time. The geological formations were combined when the lithology and geomechanical properties were of similar values. However the vertical resolution of each GMU was kept high enough so that the geomechanical properties were fairly constant with respect to depth within each GMU. The average value of the rock mechanical properties for each GMU is given in Table 3.

In Table 3 both dynamic and static Young's modulus and bulk modulus are reported, and the value of static moduli is significantly lower than the dynamic moduli. The reason for this difference is

because of the very different strain and strain rate the rock experiences in a tri-axial compressional test when compared to sonic log measurement. Similar behaviour may be expected for the dynamically measured Poisson's ratio. However the effect is less for Poisson's ratio, since the same difference will be observed for both vertical and horizontal strain measurements and will be negated when calculating Poisson's ratio. However, the results show that relying on dynamic properties alone will under predict the deformation that will occur in the formations when they are subjected to changes in stress.

Table 3: Geomechanical properties for each Geomechanical Unit (GMU).

GMU	Dominant Lithology	Depth	Thickness	Young's Module STATIC	Young's Module Dynamic	Poisson's Dynamic	Bulk Module Static	Bulk Module Dynamic	UCS	Failure Angle	Tensile Strength	Cohesion	Friction
		m	m	GPa	GPa		GPa	Gpa	MPa	°	MPa		°
Upper Colorado	Sh	1209.7	129.4	6.7	18	0.33	6.5	17.6	26	61	2.2	6.7	17
Lower Colo.	Sh	1339.1	474.5	8.1	22	0.32	7.5	20.4	32	63	2.7	8.3	19
Viking	SS	1813.6	23.9	12.2	33	0.25	8.1	22.0	39	77	3.3	10.1	39
Joli Fou	SH	1837.5	17.0	8.5	23	0.30	7.1	19.2	33	64	2.8	8.5	20
Manville	SS	1854.5	124.2	10.7	29	0.30	9.0	24.2	39	77	3.3	10.1	39
Glauc. ss	SS	1978.7	22.3	15.2	41	0.29	12.1	32.5	65	65	5.4	16.8	21
Ostracod zone	SH	2001.0	4.5	16.3	44	0.29	12.9	34.9	69	71	5.8	17.9	29
Ellerslie	SS	2005.5	16.7	13.3	36	0.22	7.9	21.4	41	77	3.4	10.6	40
Nordegg	SH	2022.2	50.6	20.7	56	0.23	12.8	34.6	106	81	8.8	27.4	47
Banff	SH	2072.8	196.5	21.5	58	0.25	14.3	38.7	87	80	7.3	22.5	45
Exhaw	SH	2269.3	4.5	15.6	42	0.21	8.9	24.1	56	69	4.7	14.5	26
Wabamun	Ca	2273.8	225.0	27.4	74	0.28	20.8	56.1	103	81	8.6	26.7	47
Blueridge	Sh	2498.8	29.4	29.3	79.0	0.29	23.2	62.7	107	75	8.9	27.7	36
Calmar – Shale	Sh	2528.2	8.0	24.8	67.0	0.27	18.0	48.6	100	75	8.3	25.9	35
Calmar Dolo-shale	Sh	2536.0	5.0	24.8	67.0	0.27	18.0	48.6	160	79	13.3	41.4	43
Nisku tight	Ca	2541.3	85.9	28.9	78.0	0.29	22.9	61.9	200	84	16.7	51.8	53
Nisku high perm	CA.			16.7	45.0	0.29	13.2	35.7	80	80	6.7	20.7	45

4. IN-SITU STABILITY OF NISKU INJECTION HORIZON

The current in-situ effective stresses for the Nisku formation is plotted as a Mohr circle in Figure 4. The effective vertical stress is approximately 26 MPa and the effective horizontal stress is approximately 20 MPa. The corresponding shear stress is low at around 3 MPa (the peak value at the Mohr circle), and the corresponding effective normal stress is 23 Mpa. Shear failure will occur when the Mohr circle intersects the failure line. Any Mohr circle below the failure line indicates a stable condition. From the graph we can also see the porous portion of the Nisku formation has a

lower failure strength than the Calmar caprock. That will help in arresting any shear fractures occurring in the porous parts from propagating through the harder Nisku and Calmar caprock.

When injection starts, the effective stresses will be reduced and the in-situ stress Mohr circle will move to the left. It is very unlikely that shear fracturing will occur during injection. The most likely scenario will be the creation of tensile hydraulic fractures, but as long as the injection pressure is kept below the lowest horizontal stress, it is unlikely that tensile fractures will occur. Since the geological model indicates that the lower portion of the Nisku is the most porous and the upper more competent parts have a higher tensile strength, any fractures will unlikely be able to migrate upwards. Since the Calmar formation is more competent than porous, it is unlikely that fractures will extend into the harder Calmar formation. This may cause hydraulic fracturing to be an attractive option to increase injectivity in the Nisku formation. However this does not consider the effect of thermal contraction in the rock caused by the injected CO_2 when its temperature is lower than the reservoir temperature. The cooling effect will reduce the least horizontal stress gradient in the cooled area, which will reduce the fracture gradient and increase the likelihood for vertical fractures to occur. Creating new shear fractures is still unlikely, since even at zero effective horizontal stress the Mohr circle in Figure 4 will not intersect any of the shear failure lines. The likelihood of fracturing the caprock due to thermal stresses is addressed in the Ggeomechanical Modelling and Analysis section.

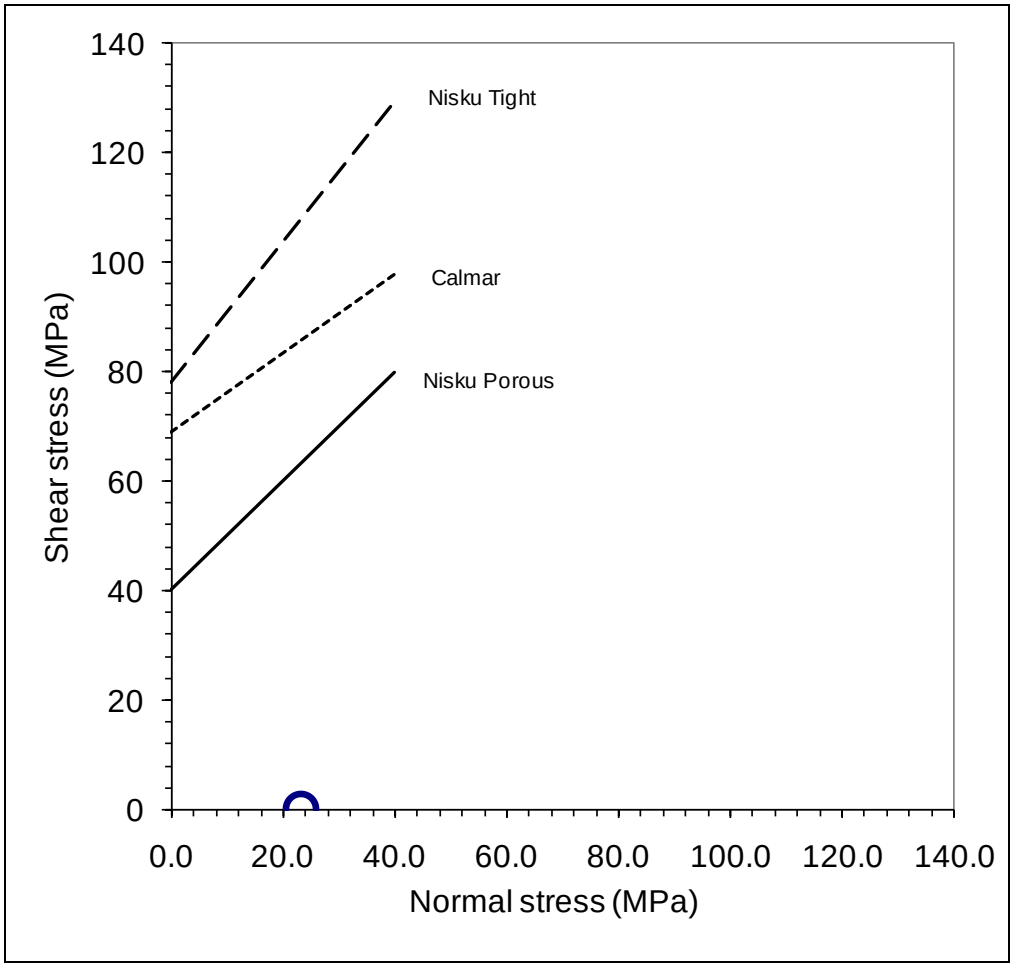

Figure 4: Mohr Diagram of existing in-situ effective stress level in the Nisku formation and the corresponding failure envelope for the reservoir and caprock.

5. CONCLUSIONS

In-situ stress characteristics for the subsurface of the Wabamun CO_2 storage area where established using existing analyses to provide guidance for maximum injection pressure, and to act as boundary conditions for further geomechanical modelling efforts.

A table of geomechanical properties for the subsurface of the Wabamun CO_2 storage area was established. Well logs were used to establish dynamic deformation properties (Young's modulus, Poisson's ratio, and bulk modulus) and correlations were used to determine static deformation properties. The unconfined compressive strength (UCS) was established for each lithology based on correlations with log properties. The database that was created was used as input for the geomechanical modelling.

The lower sedimentary succession with the Nisku aquifer and Calmar caprock is very competent and stiff rock.

A few laboratory tri-axial tests are recommended in the future to confirm the accuracy of the UCS correlations for this specific site and to adjust the dynamic-to-static conversion factors.

REFERENCES

Andrews, R., Hareland, Nygård, R., G., Engler, T. & Virginillo, B. Method of using logs to quantify drillability, Presented at; SPE Rocky Mountain Oil and Gas Technology Symposium, 16–18 April 2007, Denver, Colorado USA.

Bell, J. S., 2003, Practical methods for estimating in-situ stresses for borehole stability applications in sedimentary basins: Journal of Petroleum Science and Engineering, v. 38, no. 3-4, p.111–119.

Bell, S.J. and S. Bachu 2003, In-situ stress magnitude and orientation estimates for Cretaceous coal-bearing strata beneath the plains area of central and southern Alberta: Bulletin of Canadian Petroleum Geology, v. 51, p. 1–28.

Hareland, G., Nygård, R. 2007, Calculating unconfined rock strength from drilling data, Accepted in; 1st Canada-U.S. Rock Mechanics Symposium, 27–31 May 2007, Vancouver, British Columbia, Canada.

Kasi, A. Zekai, S. & Bahsa-Eldin, H., 1983. Relationship between Sonic Pulse Velocity and Uniaxial Compressive Strengths of Rocks. Proc. Of the 24th U.S. Symp. On Rock. Mech. Texas A&M University, 20–23 June 1983, TX, US: 409–419.

Michael, K., Bachu, S., Buschkuehle, M., Haug, K., and S. Talman. in press. Comprehensive Characterization of a Potential Site for CO_2 Geological Storage in Central Alberta, Canada, AAGP Special Publication on Carbon Dioxide Sequestration.

Onyia, E.C., 1988. Relationships Between Formation Strength, Drilling Strength, and Electric Log Properties. 63rd Ann. Tech. Conf. Houston, 2–5 October 1988, TX, USA. SPE 18166.